

## RESEARCH ARTICLE

## Implementation of Quantum Gates via Optimal Control

Sonia Schirmer<sup>a,b,\*</sup><sup>a</sup>Dept of Applied Maths and Theoretical Physics

University of Cambridge, Wilberforce Road, Cambridge, CB3 0WA, UK

<sup>b</sup>Dept of Maths and Statistics, University of Kuopio

PO Box 1627, 70211 Kuopio, Finland

*(Received 00 Month 200x; final version received 00 Month 200x)*

Starting with the basic control system model often employed in NMR pulse design, we derive more realistic control system models taking into account effects such as off-resonant excitation for systems with fixed inter-qubit coupling controlled by globally applied electromagnetic fields, as well as for systems controlled by a combination of a global fields and local control electrodes. For both models optimal control is used to find controls that implement a set of two- and three-qubit gates with fidelity  $\geq 99.99\%$ .

**Keywords:** Quantum Control Theory, Quantum Computation, Physically-realistic Control System Models, Implementation of Quantum Gates

## 1. Introduction

Controlling the dynamics of quantum systems is a problem of great recent interest with many applications from quantum chemistry to quantum computing. Since the dynamics of a quantum system is essentially determined by its Hamiltonian, a central theme in quantum control is Hamiltonian engineering. This is typically accomplished by the application of external fields, whose interaction with the system modifies its effective Hamiltonian, thereby changing its dynamical evolution. The type of control fields that are available tends to vary significantly depending on the type of system and the actuators available. In traditional applications such as nuclear spin engineering and nuclear magnetic resonance (NMR), the fields are often radiofrequency pulses, while in applications involving transitions between electronic states in atoms or vibrational modes of molecules, the control fields are usually laser pulses. In more recent applications such as various solid-state architectures based on semi-conductor quantum dots or Josephson junctions, the controls are often electric fields produced by external electrodes. Despite the disparate physical realizations, all of these applications share important similarities, in that the external fields modify the Hamiltonian in a certain way, and the objective generally is to find a particular control that modifies the dynamics in a certain way, and achieves a certain objective, e.g., of steering the system to a particular state or realizing a desired quantum process.

There are many differences in the specifics, however, which can be very important for the design of effective and experimentally feasible controls. In NMR applications, for example, we can often approximate the system well by assuming that the control fields induce rapid local rotations of individual spins, which interact through a fixed, weak coupling between them that is not affected by the control fields. Furthermore, we can often assume that we can selectively address individual spins by frequency-selective control pulses, and that we can perform local rotations about orthogonal axes. The same approximations, however, are not necessarily valid for other systems such as solid-state architectures. In particular for systems controlled by local voltage gates, it is often difficult to perform rotations about orthogonal axes, and a voltage applied to a local electrode may have non-negligible effects on the dynamics of nearby quantum dots, and in the presence of multiple control voltages there can be significant cross-talk effects, all of which can significantly complicate effective control design. In this paper we attempt to incorporate some of these effects to derive more realistic control system models for two types of systems of practical interest, and apply optimal control theory to find control solutions to implement a set of elementary gates for the resulting more complex control system models.

\*Corresponding author. Email: sgs29@cam.ac.uk

## 2. Basic NMR control system model and geometric control

The starting point for many optimal control problems in quantum computing such as optimal implementation of quantum gates has often been a control system model inspired by liquid-state nuclear magnetic resonance (NMR). Using the common shorthand  $\hat{\sigma}_k^{(n)}$  to denote an  $N$ -factor tensor product in which the  $n$ th factor is the Pauli matrix  $\hat{\sigma}_k$  for  $k \in \{x, y, z\}$  and all other factors are the identity I, the Hamiltonian for a system consisting of  $N$  spin- $\frac{1}{2}$  nuclei (qubits) in this model is usually given by

$$\hat{H}[\mathbf{u}(t)] = \hbar \sum_{n < n'} J_{nn'} \hat{\sigma}_z^{(n)} \hat{\sigma}_z^{(n')} + \hbar \sum_{n=1}^N \left( u_{2n-1}(t) \hat{\sigma}_x^{(n)} + u_{2n}(t) \hat{\sigma}_y^{(n)} \right), \quad (1)$$

where the first term is a fixed inter-qubit coupling term, in this case of Ising type, and we have  $2N$  independent control fields  $u_{2n-1}(t)$  and  $u_{2n}(t)$  capable of performing local  $x$  and  $y$  rotations on the  $n$ th spin, respectively.

If the interqubit couplings  $J_{nn'}$  are controllable, or at least can be switched off, then it is very easy to see that we can implement any local unitary operation  $\hat{U} \in \mathfrak{SU}(2)$  on the  $n$ th qubit, e.g., by performing a sequence of three local rotations about the orthogonal axes  $\hat{\sigma}_x^{(n)}$  and  $\hat{\sigma}_y^{(n)}$ , e.g., using the standard Euler decomposition  $\hat{U} = \hat{U}_x(\alpha) \hat{U}_y(\beta) \hat{U}_x(\gamma)$  with  $\hat{U}_x(\alpha) = \exp(-i\alpha \hat{\sigma}_x)$ , etc, for suitable values of the rotation angles  $\alpha, \beta, \gamma$ , and two-qubit gates can be implemented using the Cartan decomposition (2, 3, 4),

$$\hat{U} = \hat{U}_1 [\hat{U}_y \hat{Z}(\alpha_3) \hat{U}_y^{-1}] [\hat{U}_x^{-1} \hat{Z}(\alpha_2) \hat{U}_x] \hat{Z}(\alpha_1) \hat{U}_2, \quad (2)$$

where  $\hat{Z}(\alpha) = \exp(-i\alpha \hat{\sigma}_z^{(1)} \hat{\sigma}_z^{(2)})$  corresponds to free evolution under the Ising-coupling Hamiltonian for a suitable time,  $\hat{U}_1$  and  $\hat{U}_2$  correspond to local operations on both qubits, which can be implemented using the Euler decomposition, and  $\hat{U}_x = \hat{U}_x^{(1)}(\frac{\pi}{4}) \otimes \hat{U}_x^{(2)}(\frac{\pi}{4})$  correspond to local  $x$ -rotations by  $\frac{\pi}{4}$  on both qubits, and similarly for  $\hat{U}_y$ .

If the inter-qubit coupling terms  $J_{nn'}$  are fixed and not controllable then this gives rise to a drift term, which complicates the situation. If the coupling is weak and we can apply ‘‘hard pulses’’, e.g., if we can ensure

$$\sqrt{u_{2n-1}^2 + u_{2n}^2} \gg \max_{n'} |J_{nn'}|,$$

then the drift term is negligible (as far as the implementation of local gates is concerned), and the geometric control pulse sequences derived from the Euler and Cartan decomposition are often a good approximation. However, if the coupling is stronger or hard pulses are not available, neglecting the drift term will result in inaccurate gates. Moreover, in realistic applications, hard pulses may lead to other problems such as off-resonant excitation.

Although we can in principle try to find geometric decompositions that take the drift term into account (5), geometric control pulse sequences derived from Lie group decompositions are usually not optimal even when the drift is negligible, and optimal control has been shown to be able to produce more effective or efficient control pulses with regard to various performance indices such as gate operation times or average fidelity even for cases where geometric decompositions are valid, at least theoretically [See e.g. (6)].

## 3. Realistic control system models for optimal control

The success of optimal control theory in finding more effective control pulse sequences for various model problems has fueled a surge of interest in this area. However, the control system models on which many of the optimal control calculations so far have been based are generally too simple and often unrealistic for the systems they are supposed to model. The model described in the previous section, for example, is based on many approximations that may be questionable even in NMR settings, and certainly for other applications. For instance, in the ideal case the control fields  $u_{2n-1}(t)$  and  $u_{2n}(t)$  induce only an  $x$ -rotation and  $y$ -rotation, respectively, on the  $n$ th qubit, but the desire to speed up gate implementation times may produce strong control fields likely to induce off-resonant excitations not accounted for in the model.

Off-resonant excitation means that the fields are not only felt by the target qubit but also by other qubits. In the simplest case we can try to model off-resonant excitation by replacing the individual interaction Hamiltonians  $\hat{\sigma}_x^{(n)}$  and  $\hat{\sigma}_y^{(n)}$  for the independent control

fields  $u_{2n-1}(t)$  and  $u_{2n}(t)$  by linear combinations of the coupling terms

$$\hat{\sigma}_x^{(n)} \mapsto \hat{H}_{2n-1} = \sum_{n'} \alpha_{2n-1,2n'-1} \hat{\sigma}_x^{(n')} + \alpha_{2n-1,2n'} \hat{\sigma}_y^{(n')}, \quad (3a)$$

$$\hat{\sigma}_y^{(n)} \mapsto \hat{H}_{2n} = \sum_{n'} \alpha_{2n,2n'-1} \hat{\sigma}_x^{(n')} + \alpha_{2n,2n'} \hat{\sigma}_y^{(n')}. \quad (3b)$$

The new interaction Hamiltonians  $\hat{H}_m$  for  $m = 1, \dots, 2N$  no longer correspond to local rotations about mutually orthogonal axes, which makes finding geometric decompositions for this case very challenging in general. However, even arbitrary (linear) cross-talk need not be an obstacle for optimal control as shown in (7) for a model system of this type. Provided the cross-talk Hamiltonians are known, based on a combination of theoretical models and experimental characterization, it still appears to easy to find effective control pulses using optimal control algorithms. The main drawback is that this simple model does not accurately model real cross-talk.

### 3.1. Control via globally applied fields with off-resonant excitation

The intrinsic system Hamiltonian for a system of  $N$  spins with resonance frequencies  $\omega_n$  with static Ising coupling  $J_{nn'}$  in a fixed laboratory frame is

$$\hat{H}_0 = \hbar \sum_{n < n'} J_{nn'} \hat{\sigma}_z^{(n)} \hat{\sigma}_z^{(n')} - \hbar \sum_n \frac{\omega_n}{2} \hat{\sigma}_z^{(n)}. \quad (4)$$

If we apply a global electromagnetic field  $\mathbf{B}(t)$  with components  $B_x(t) = B(t) \cos(\omega t + \phi)$  and  $B_y(t) = B(t) \sin(\omega t + \phi)$ , respectively, the resulting control Hamiltonian is

$$\hat{H}_c = -\frac{\hbar}{2} \sum_n \gamma_n B(t) [\cos(\omega t + \phi) \hat{\sigma}_x^{(n)} - \sin(\omega t + \phi) \hat{\sigma}_y^{(n)}] \quad (5)$$

Transforming to a multiply rotating frame defined by  $\hat{U}_S(t) = \exp(-i \frac{t}{2} \sum_n \omega_n \hat{\sigma}_z^{(n)})$ , the interaction picture rotating wave approximation Hamiltonian is (1)

$$\hat{H} = \hbar \sum_{n,n'} J_{nn'} \hat{\sigma}_z^{(n)} \cdot \hat{\sigma}_z^{(n')} - \frac{\hbar}{2} \sum_n \gamma_n B(t) [\cos(\Delta\omega_n t + \phi) \hat{\sigma}_x^{(n)} - \sin(\Delta\omega_n t + \phi) \hat{\sigma}_y^{(n)}] \quad (6)$$

where  $\Delta\omega_n = \omega - \omega_n$  and  $\Omega_n(t) = \gamma_n B(t)$ . If the field is exactly resonant with the  $n$ th spin,  $\omega = \omega_n$ , then the term corresponding to the  $n$ th spin simplifies to

$$-\frac{\hbar}{2} \gamma_n B(t) [\cos(\phi) \hat{\sigma}_x^{(n)} - \sin(\phi) \hat{\sigma}_y^{(n)}].$$

If we can further argue that all other spins have frequencies  $\omega_n$  far detuned from  $\omega$ ,  $|B(t)|$  is slowly varying and not too large,  $|\gamma_{n'} B(t)| \ll |\Delta\omega_{n'}|$  for all  $n' \neq n$ , then for sufficiently large  $T$  the rapidly oscillating terms will “average to zero”, i.e., we can assume

$$\begin{aligned} \frac{1}{T} \int_0^T B(t) \gamma_{n'} \cos(\Delta\omega_{n'} t + \phi) dt &\approx 0 \\ \frac{1}{T} \int_0^T B(t) \gamma_{n'} \sin(\Delta\omega_{n'} t + \phi) dt &\approx 0. \end{aligned}$$

In this case the effective control Hamiltonian associated with the field  $\mathbf{B}(t)$  simplifies to

$$\hat{H}_c = -\frac{\hbar}{2} \Omega_n(t) [\cos(\phi) \hat{\sigma}_x^{(n)} - \sin(\phi) \hat{\sigma}_y^{(n)}].$$

Thus, if we are able to simultaneously apply  $N$  independent fields  $B_x^{(n)}(t) \cos(\omega_n t)$  with frequencies  $\omega_n$  and  $N$  independent fields  $B_y^{(n)}(t) \sin(\omega_n t)$  with frequencies  $\omega_n$ , for instance, then assuming all the previous assumptions and approximations still hold, we obtain

$$\hat{H} = \hbar \sum_{n,n'} J_{nn'} \hat{\sigma}_z^{(n)} \cdot \hat{\sigma}_z^{(n')} - \frac{\hbar}{2} \sum_n [B_x^{(n)}(t) \gamma_n \hat{\sigma}_x^{(n)} - B_y^{(n)}(t) \gamma_n \hat{\sigma}_y^{(n)}], \quad (7)$$

exactly the Hamiltonian (1) with  $u_{2n-1}(t) = -\frac{1}{2}\gamma_n B_x^{(n)}(t)$  and  $u_{2n}(t) = \frac{1}{2}\gamma_n B_y^{(n)}(t)$ .

In practice, it is questionable, however, whether these approximations are still valid in general, especially if we simultaneously apply  $2N$  control fields  $B_x^{(n)}(t)$  and  $B_y^{(n)}(t)$ , all of which may be strongly modulated in time as a result of an optimization procedure, and thus not slowly varying. Furthermore, the interaction picture RWA Hamiltonian (6) is not a very good starting point for a general optimization either because each of the independent control Hamiltonians

$$\hat{H}_m(t) = -\frac{\hbar}{2} \sum_n \gamma_n [\cos(\Delta\omega_{n,m}t + \phi_m) \hat{\sigma}_x^{(n)} - \sin(\Delta\omega_{n,m}t + \phi_m) \hat{\sigma}_y^{(n)}] \quad (8)$$

with  $\omega_{n,m} = \omega_m - \omega_n$  for a field  $\mathbf{B}_m(t)$  with  $B_x(t) = B_m(t) \cos(\omega_m t + \phi_m)$  and  $B_y(t) = B_m(t) \sin(\omega_m t + \phi_m)$ , in the total Hamiltonian

$$\hat{H} = \hat{H}_0 + \sum_m B_m(t) \hat{H}_m(t) \quad (9)$$

is time-dependent, containing rapidly oscillating sine and cosine terms. Therefore, we might as well let the component functions  $B_x(t)$  and  $B_y(t)$  of the field be completely arbitrary and work with the general Hamiltonian

$$\hat{H} = \hat{H}_0 - B_x(t) \frac{\hbar}{2} \sum_n \gamma_n \hat{\sigma}_x^{(n)} + B_y(t) \frac{\hbar}{2} \sum_n \gamma_n \hat{\sigma}_y^{(n)} \quad (10)$$

with  $\hat{H}_0$  as in Eq. (4), instead.

### 3.2. Control via fixed global fields and local control electrodes

In some applications such as NMR the only type of control we have is globally applied control fields. However, for many systems, especially solid-state systems such as the nuclear spins of donor atoms embedded in a substrate (8), or electron spins in quantum dots (9), for example, some local control in the form of control electrodes is available, and in a typical setting, control is achieved by combining globally applied electromagnetic fields with local fields provided by control electrodes (10). In this case we often have a global electromagnetic field  $\mathbf{B}(t)$  with components  $B_x(t) = B(t) \cos(\omega t)$ ,  $B_y(t) = B(t) \sin(\omega t)$ , in addition to a static magnetic field in the  $z$  direction, and a Hamiltonian of the form

$$\begin{aligned} \hat{H} = & \hbar \sum_{n < n'} J_{nn'} \hat{\sigma}^{(n)} \cdot \hat{\sigma}^{(n')} - \frac{\hbar}{2} \sum_n \omega_n(\mathbf{V}) \hat{\sigma}_z^{(n)} \\ & - \frac{\hbar}{2} \sum_n \gamma_n B(t) [\cos(\omega t) \hat{\sigma}_x^{(n)} - \sin(\omega t) \hat{\sigma}_y^{(n)}], \end{aligned} \quad (11)$$

as before, but in addition we now have some degree of control over the resonance frequency  $\omega_n$  of the  $n$ th qubit via local control electrodes. Note that unlike in the previous model we have assumed isotropic Heisenberg coupling, i.e.,

$\hat{\sigma}^{(n)} \cdot \hat{\sigma}^{(n')} = \hat{\sigma}_x^{(n)} \hat{\sigma}_x^{(n')} + \hat{\sigma}_y^{(n)} \hat{\sigma}_y^{(n')} + \hat{\sigma}_z^{(n)} \hat{\sigma}_z^{(n')}$ , instead of  $\hat{\sigma}_z^{(n)} \hat{\sigma}_z^{(n')}$ . Ising coupling as this seems to be more appropriate for solid-state systems, although the assumption of isotropy may not be appropriate for some systems.

One control approach is to simultaneously vary the voltages applied to the local control electrodes as well as the globally applied field. However, in practice it is much simpler to apply a global field  $\mathbf{B}(t)$  with a fixed amplitude  $B$  and fixed frequency  $\omega$  and only vary the voltages applied to the local control electrodes. In this case we can introduce a rotating frame, this time rotating at the field frequency  $\omega$ ,  $\hat{U}_S(t) = \exp(-i\frac{t}{2} \sum_n \omega \hat{\sigma}_z^{(n)})$ , to obtain the slightly simpler interaction picture Hamiltonian

$$\hat{H} = \hbar \sum_{n < n'} J_{nn'} \hat{\sigma}^{(n)} \cdot \hat{\sigma}^{(n')} - \frac{\hbar}{2} \sum_n \omega_n(\mathbf{V}) \hat{\sigma}_z^{(n)} - \hbar \Omega \sum_n \tilde{\gamma}_n \hat{\sigma}_x^{(n)}, \quad (12)$$

where we set  $\Omega = \frac{1}{2}B\gamma_0$  and take  $\tilde{\gamma}_n$  to be the coupling constants  $\gamma_n$  in units of some coupling strength  $\gamma_0$ , so that for a homogeneous system consisting of a chain of spins that couple identically to the field we have  $\tilde{\gamma}_n = 1$  for  $n > 0$ .

In this model the constants  $J_{nn'}$  and  $\gamma_n$  are usually fixed and determined by the physics of the system. The frequency  $\omega$  and Rabi frequency  $\Omega$  of the field can be chosen initially but are then fixed. Thus, all the dynamic control is achieved by dynamically changing the

control voltages and thus  $\omega_n(\mathbf{V})$ . This type of control therefore leads to a different partitioning of the total Hamiltonian into a fixed drift and variable control part

$$\begin{aligned}\hat{H}_0 &= \hbar \sum_{n < n'} J_{nn'} \hat{\sigma}^{(n)} \cdot \hat{\sigma}^{(n')} - \hbar \Omega \sum_n \bar{\gamma}_n \hat{\sigma}_x^{(n)}, \\ \hat{H}_c &= -\frac{\hbar}{2} \sum_n \omega_n(\mathbf{V}) \hat{\sigma}_z^{(n)}.\end{aligned}$$

In general, due to cross-talk effects (11) the energy level shift of the  $n$ th qubit may be a complicated function of all the voltages applied, not only to the electrode directly above it, but to neighbouring control electrodes as well, i.e.,  $\omega_n$  may be a function of all the control voltages  $\mathbf{V} = (V_1, \dots, V_m)$  applied, i.e.,  $\omega_n = \omega_n(\mathbf{V})$ .

## 4. Optimal gate implementation

### 4.1. Optimal control formulation

One way to solve the problem of finding controls  $\mathbf{u}(t)$  that implement a desired set of quantum gates, especially for control systems that are not amenable to simple geometric decomposition schemes, such as the ones discussed in the previous section, is to formulate the task as an optimization problem. This typically involves (a) choosing a target function to be optimized, (b) finding a suitable parametrization for the set of admissible (and experimentally feasible) controls, and (c) finding a solution to the resulting, possibly constrained, optimization problem based on application of Pontryagin's maximum principle (12).

For the task of implementation of quantum gates or processes, a natural choice for the objective function is the gate fidelity (13)

$$\mathcal{F}(\hat{U}_T, \hat{U}) = \frac{1}{N} \Re \text{Tr}(\hat{U}_T^\dagger \hat{U}). \quad (13)$$

The reason for the factor of  $1/N$ , where  $N$  is the system dimension, is to ensure that  $\mathcal{F}$  varies between  $-1$  (for  $\hat{U} = -\hat{U}_T$ ) and  $+1$  (for  $\hat{U} = \hat{U}_T$ ) independent of the system dimension. In general, maximizing the gate fidelity is equivalent to minimizing the gate error

$$\mathcal{E}(\hat{U}_T, \hat{U}) = \|\hat{U} - \hat{U}_T\|^2. \quad (14)$$

This is very to see if the target operator  $\hat{U}_T$  and the actual operator  $\hat{U}$  are both unitary (and thus  $\hat{U}^\dagger \hat{U} = \hat{U}_T^\dagger \hat{U}_T = \hat{I}$ ) as

$$\begin{aligned}\|\hat{U} - \hat{U}_T\|^2 &= \text{Tr}[(\hat{U} - \hat{U}_T)^\dagger (\hat{U} - \hat{U}_T)] \\ &= \text{Tr}[\hat{U}^\dagger \hat{U} + \hat{U}_T^\dagger \hat{U}_T - \hat{U}^\dagger \hat{U}_T - \hat{U}_T^\dagger \hat{U}] \\ &= 2N - 2\Re \text{Tr}(\hat{U}_T^\dagger \hat{U}).\end{aligned}$$

Noting that the implemented operator  $\hat{U} = \hat{U}_{\mathbf{u}}(t_F)$  is a function of the control  $\mathbf{u}$ , the control objective is to find an admissible control  $\mathbf{u}_{\text{opt}}$  such that

$$\mathcal{F}(\hat{U}_T, \hat{U}_{\mathbf{u}_{\text{opt}}}(t_F)) = \max_{\mathbf{u} \in \mathcal{A}} \mathcal{F}(\hat{U}_T, \hat{U}_{\mathbf{u}}(t_F)), \quad (15)$$

and of course,  $\hat{U}_{\mathbf{u}}(t)$  has to satisfy the Schrodinger equation

$$\frac{d}{dt} \hat{U}_{\mathbf{u}}(t) = -\frac{i}{\hbar} \hat{H}[\mathbf{u}(t)] \hat{U}_{\mathbf{u}}(t), \quad (16)$$

where  $\hat{H}[\mathbf{u}(t)]$  is the control-dependent Hamiltonian of the system.

### 4.2. Iterative control optimization algorithm

Once the Hamiltonian  $\hat{H}[\mathbf{u}(t)]$ , the target time  $t_F$  and the target operator  $\hat{U}_T$  have been chosen, the fidelity depends only on the choice of the control  $\mathbf{u}(t)$ , i.e.,  $\mathcal{F} = \mathcal{F}_{\mathbf{u}}$ . Now let  $\mathbf{u}$

and  $\mathbf{u} + \Delta\mathbf{u}$  be two controls. Noting that

$$\delta\hat{U}_{\mathbf{u}}(t) := \hat{U}_{\mathbf{u}+\Delta\mathbf{u}}(t) - \hat{U}_{\mathbf{u}}(t) = \int_{t_0}^t \hat{U}_{\mathbf{u}}(t, \tau) \hat{D}_{\Delta\mathbf{u}}(\tau) d\tau \quad (17)$$

and that for a control-linear Hamiltonian  $\hat{H}[\mathbf{u}(t)] = \hat{H}_0 + \sum_m u_m(t) \hat{H}_m$  we have

$$\hat{D}_{\Delta\mathbf{u}}(t) = -\frac{i}{\hbar} \sum_m \Delta u_m(t) \hat{H}_m \hat{U}_{\mathbf{u}+\Delta\mathbf{u}}(t) \quad (18)$$

we obtain immediately

$$\begin{aligned} \Delta\mathcal{F} &= \mathcal{F}_{\mathbf{u}+\Delta\mathbf{u}} - \mathcal{F}_{\mathbf{u}} \\ &= \frac{2}{N} \Re \text{Tr} [\hat{U}_T^\dagger (\hat{U}_{\mathbf{u}+\Delta\mathbf{u}}(t) - \hat{U}_{\mathbf{u}}(t))] \\ &= \frac{2}{N\hbar} \Im \text{Tr} \left[ \hat{U}_T^\dagger \int_{t_0}^{t_F} \hat{U}_{\mathbf{u}}(t_F, t) \sum_m \Delta u_m(t) \hat{H}_m \hat{U}_{\mathbf{u}+\Delta\mathbf{u}}(t) dt \right] \\ &= \frac{2}{N\hbar} \sum_m \int_{t_0}^{t_F} \Delta u_m(t) \Im \text{Tr} \left[ \hat{U}_T^\dagger \hat{U}_{\mathbf{u}}(t_F, t) \hat{H}_m \hat{U}_{\mathbf{u}+\Delta\mathbf{u}}(t) \right] dt \end{aligned}$$

which shows that setting

$$\Delta u_m(t) = \epsilon_m(t) \Im \text{Tr} \left[ \hat{U}_T^\dagger \hat{U}_{\mathbf{u}}(t_F, t) \hat{H}_m \hat{U}_{\mathbf{u}+\Delta\mathbf{u}}(t) \right] \quad (19)$$

with  $\epsilon_m(t) > 0$  for all  $t$  will increase the fidelity. Thus, starting with any initial guess  $\mathbf{u}_0(t)$ , iteratively solving the Schrodinger equation while updating the control in each iteration according to the rule  $\mathbf{u}^{(n+1)} = \mathbf{u}^{(n)} + \Delta\mathbf{u}^{(n)}$ , with  $\Delta\mathbf{u}^{(n)}$  chosen as in Eq. (19), will monotonically increase the fidelity in each iteration, and as the fidelity is of course bounded, the iteration must converge to some limiting fidelity  $\mathcal{F}^\infty$ , although we cannot guarantee that the limiting value will be equal to the global maximum of the fidelity. In fact, many optimal control algorithms are based precisely on this iterative update scheme.

### 4.3. Parametrization of controls and discretization

To solve the Schrodinger equation numerically, we still require some discretization. The simplest approach is to assume piecewise constant fields  $\mathbf{u}(t) = \mathbf{u}_k$  for  $t_{k-1} \leq t \leq t_k$ , in which case the exact solution of the Schrodinger equation is explicitly

$$\hat{U}_{\mathbf{u}}(t_F) = \hat{U}_{\mathbf{u}_K}(\Delta t_K) \hat{U}_{\mathbf{u}_{K-1}}(\Delta t_{K-1}) \dots \hat{U}_{\mathbf{u}_1}(\Delta t_1) \quad (20)$$

where  $\Delta t_k = t_k - t_{k-1}$ ,  $t_K = t_F$ , and

$$\hat{U}_{\mathbf{u}_k}(\Delta t_k) = \exp \left[ -\frac{i}{\hbar} \Delta t_k \hat{H}(\mathbf{u}_k) \right] \quad (21)$$

is a simple matrix exponential and the update rule becomes

$$\Delta u_m(t_k) = \epsilon_m(t) \Im \text{Tr} \left[ \hat{U}_T^\dagger \hat{U}_{\mathbf{u}_K}(t_K) \dots \hat{U}_{\mathbf{u}_{k+1}}(t_{k+1}) \hat{H}_m \hat{U}_{\mathbf{u}_k}(\Delta t_k) \dots \hat{U}_{\mathbf{u}_1}(\Delta t_1) \right]. \quad (22)$$

With this type of discretization there are two ways of implementing the update rule. In the global update approach all the matrix exponentials for all times  $t_k$  are evaluated to solve the Schrodinger equation, and the fields are updated for all times  $t_k$  simultaneously at the end of each iteration step. This is essentially the well-known GRAPE algorithm as described in (14). An alternative is to update the fields  $u_m(t_k)$  at each time step  $t_k$ . Our analysis above shows that both approaches will monotonically increase the fidelity provided  $\epsilon_m(t_k) > 0$  for all  $t_k$ , although they will tend to converge to different solutions for the fields.

In our limited numerical experiments for the systems considered here, both approaches seemed equally effective in finding satisfactory control fields but the local update approach tended to converge faster in terms of the computational time required to find a solution. The main reason for this appears to be that in the local update approach only a single  $\mathbf{u}_k$  is incremented at a time, and hence we can optimize the multiplier  $\epsilon_k$  with very little computational overhead to speed up the convergence, as any local change of  $\epsilon_k$  requires only

re-evaluation of a single matrix exponential (and two matrix multiplications and a trace operation) to assess its effect on the fidelity, while in the global update any change in  $\epsilon$  requires the re-evaluation of all the  $K$  matrix exponentials and  $K - 1$  matrix multiplications to assess the fidelity of the new control. An alternative to this simple step-size control is to use higher derivatives to predict the optimal step-size but this also involves potentially significant computational overhead to find the best step size, in addition to the need to calculate analytical expressions for these derivatives, thus it is not clear if this will yield a computational advantage or not, although it is worth investigating.

A general shortcoming of this simple optimization procedure is that it does not take constraints into account or include penalties for less desirable fields. Simple constraints such as upper bounds on the field amplitudes can easily be incorporated into the algorithm. More complex constraints such as limiting the frequency bandwidth of pulses or minimizing the overall pulse energies etc require augmentation of the objective functional by constraint or penalty terms and modifications to the update rules. For some types of penalty terms iterative algorithms very similar to the algorithm above exist [see e.g. (15)], but a detailed discussion of appropriate penalty functions, resulting iterative update rules, and comparison of the resulting optimal fields is beyond the scope of this paper.

## 5. Simulation details and results

The specific task we wish to accomplish here is finding controls  $\mathbf{u}(t)$  that implement the following complete set of universal gates (i.e., target operators)

$$\hat{U}_T \in \{I \otimes I, \text{Had} \otimes I, T \otimes I, I \otimes \text{Had}, I \otimes T, \text{CNOT}\} \quad (23)$$

for a two-qubit system, where we employ the common approximations  $\text{Had} = \exp(i\frac{\pi}{4}Y)$ ,  $T = \exp(i\frac{\pi}{8}Z)$  and  $\text{CNOT} = e^{-i\pi/4} \text{diag}(I, X)$ . The phase factor for the CNOT is necessary to ensure that the target operators are in  $\mathfrak{SU}(4)$  since our model Hamiltonians have zero trace and hence can only generate operators in  $\mathfrak{SU}(4)$ . As a second, more challenging task we consider the implementation of the Toffoli-like three-qubit gate

$$\hat{U}_T = \text{diag}(1, 1, 1, 1, 1, 1, iX) \in \mathfrak{SU}(8). \quad (24)$$

For the simulations we assume uniform nearest-neighbour coupling, i.e.,  $J_{nn'} = J\delta_{n,n'-1}$ . Since the coupling constants  $J$  in our model have units of frequency, by choosing time in units of  $1/J$ , we can set the coupling constants to unity. All other frequencies, unless otherwise stated, are also chosen in units of  $J$ . We can furthermore choose the units of energy such that  $\hbar$ , which has units of energy  $\times$  time, equals 1, and can thus be omitted. For the two-qubit gates we set the target gate operation time to  $t_F = 1$ , while for the three-qubit gate we choose  $t_F = 5$  as a Toffoli gate normally requires five two-qubit gates. We choose these values as reasonable target times although we were able to find solutions for smaller  $t_F$  for many gates, suggesting that the gate operation times could in fact be improved.

### 5.1. Global control fields with off-resonant excitation

For our first model system with Hamiltonian (10), assuming  $\gamma_n = \gamma_0$  for all  $n$ , and setting  $u_1(t) = -\frac{1}{2}\gamma_0 B_x(t)$  and  $u_2(t) = \frac{1}{2}\gamma_0 B_y(t)$ , the Hamiltonian becomes

$$\hat{H} = ZZ - \frac{1}{2}(\omega_1 ZI + \omega_2 IZ) + u_1(t)(XI + IX) + u_2(t)(YI + IY) \quad (25)$$

for a two-qubit system, and for a three-qubit system we have

$$\begin{aligned} \hat{H} = & (ZZI + IZZ) - \frac{1}{2}(\omega_1 ZII + \omega_2 IZI + \omega_3 IIZ) \\ & + u_1(t)(XII + IXI + IIX) + u_2(t)(YII + IYI + IYY). \end{aligned} \quad (26)$$

Fig. 1 shows the actual control field solutions for a system with  $\omega_1 = 10$  and  $\omega_2 = 12$ , i.e., a system with Ising coupling frequency about 10% of the smaller qubit frequency, i.e., strong enough to be non-negligible for single qubit operations, and a qubit frequency difference large enough to allow some selectivity but still small enough so that off-resonant excitation is a concern for pulses of the magnitude and duration required for to achieve the desired gate operation times. For this model system we choose a relatively large number of time steps,  $K = 100$ , motivated by the assumption that the  $x$  and  $y$  components of the globally applied electromagnetic field could be varied more or less arbitrarily, although simulations suggest that we can find piecewise constant solutions with much fewer steps, if necessary.

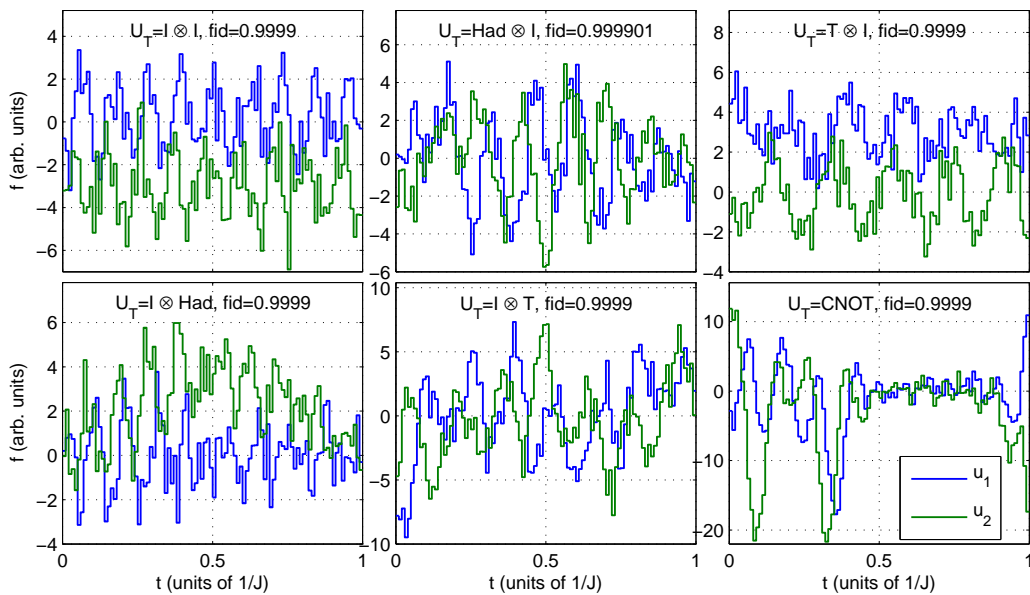


Figure 1. Control field solutions for system (25) with  $\omega_1 = 10$  and  $\omega_2 = 12$  for elementary gates (23) and  $t_f = 1$  with 100 time steps and no field constraints.

The solutions are not unique and in fact different initial fields or update rules generally produce different solutions. Again, despite the increased complexity of the model (off-resonant excitation, no RWA) and the reduced number of control fields (two vs four in the simpler model (1)), it appeared easy to find solutions that achieved the target fidelity of  $\geq 0.9999$ , or gate errors  $\leq 0.01\%$ . However, as the figure shows, the magnitudes of the fields for at least some of the gates are relatively large. Further analysis also shows that the spectral range of the optimal controls produced by this algorithm tends to be rather broad, which may be a concern in practice when there are bandwidth limitations as filtering of high or low frequency components will reduce the gate fidelity. Some numerical simulations for related problems suggest that solutions with much lower spectral bandwidth often exist but it appears that a different parametrization of the fields and optimization approach are required to find such solutions. Finding controls to implement the three-qubit gate proved more of a challenge for this system, in part because convergence was extremely slow. Fig. ??(left) shows a solution with fidelity  $\geq 99.99\%$ . Notice that the fields have high amplitudes and are very noisy. Fig. 4(left) also shows that the fields have very large spectral bandwidth as expected, which would make faithful implementation in the laboratory challenging.

## 5.2. Control via fixed global fields and local control electrodes

For our second model system with Hamiltonian (12), assuming again  $\gamma_n = \gamma_0$  for all  $n$ , and setting  $u_n(t) = -\frac{1}{2}\omega_n(\mathbf{V}(t))$  for  $n = 1, \dots, N$ , the Hamiltonian becomes

$$\hat{H} = XX + YY + ZZ - \Omega(XI + IX) + u_1(t)ZI + u_2(t)IZ \quad (27)$$

for a two-qubit system, and for a three-qubit system we have

$$\begin{aligned} \hat{H} = & (XXI + YYI + ZZI + IXX + IYY + IZZ) - \Omega(XII + IXI + IIX) \\ & + u_1(t)ZII + u_2(t)IZI + u_3IIZ. \end{aligned} \quad (28)$$

Notice that we take  $u_n(t)$  to be independent controls here to circumvent the complex and highly architecture specific problem of mapping the actual control voltages  $\mathbf{V}$  onto the frequency shifts  $\omega_n(\mathbf{V})$ , although it must be stressed that optimal control solutions for  $\mathbf{u}(t)$  will only be useful for a specific system if the  $\mathbf{u}(t)$  can be actually realized through proper choice of the voltages, which is likely to impose additional, non-trivial constraints.

Again, we chose target gate operation times of  $t_F = 1$  and  $t_F = 5$  for the two- and three-qubit gates, respectively, but in this case we tried to minimize the number of steps  $K$ , assuming that frequent switching of the control voltages would be experimentally more challenging and increase errors. As Fig. 2 shows for  $\Omega = 10$  (in units of  $J$ ) we were able to find satisfactory solutions for all six two-qubit gates with only  $K = 10$  switches. We note that  $\Omega \approx 10$  appeared to be optimal in the sense that we had to increase  $K$  significantly for



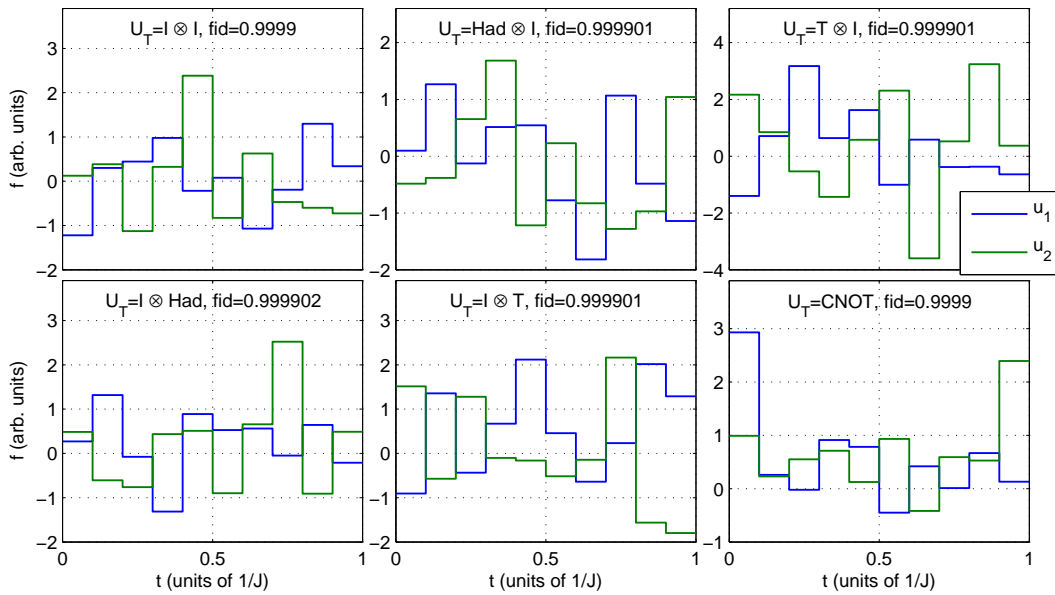


Figure 2. Control field solutions for system (27) with  $\Omega = 10$  for elementary gates (23) and  $t_f = 1$  with 10 time steps and no field constraints.

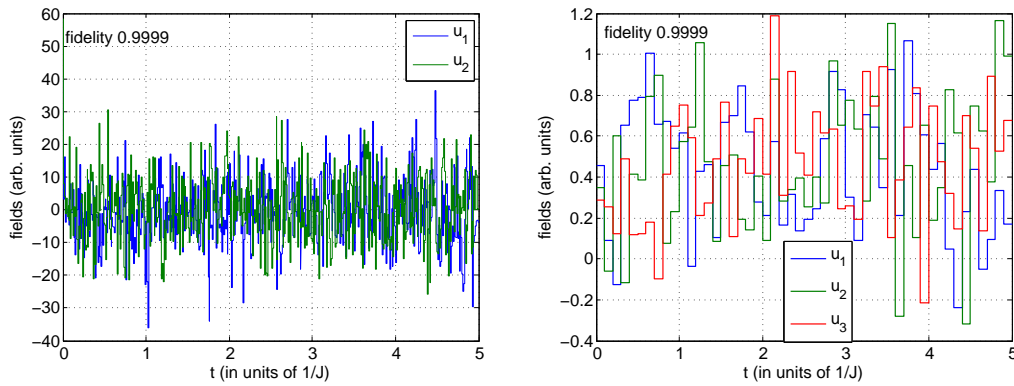


Figure 3. Control field solutions for three-qubit Toffoli-like gate for model system (26) with  $\omega_1 = 10$ ,  $\omega_2 = 12$  and  $\omega_3 = 8$  (left), and model system (28) with  $\Omega = 10$  (right).

larger or smaller values of  $\Omega$ . For  $\Omega = 1$ , for example, we had to increase the number of steps to  $K = 40$  and double the target time to be able to implement the first five two-qubit gates (corresponding to local operations) with fidelity  $\geq 0.9999$ , and for the final CNOT gate the fidelity we achieved was still only 0.9996, i.e., below threshold. For  $\Omega = 5$  we were able to find solutions above threshold fidelity for all target gates for  $K = 20$ ; for  $K = 10$  the fidelity of the CNOT gate remained below threshold (99.33%). Similarly, for  $\Omega = 20$  we were able to find solutions above the threshold fidelity for all gates for  $K = 20$  but not for  $K = 10$ . For even larger  $\Omega$ , such as 30 or 40,  $K$  had to be increased to 30, and for  $\Omega$  in the 50-60 range  $K = 50$  steps were required. These results can be partially explained considering that if  $\Omega$  is on the order of the fixed coupling strengths then the weight of the drift term makes it harder to implement local operations hence the increase in the time required. For large  $\Omega$  local operations become easier to implement but entangling gates such as the CNOT, which rely on generation of entanglement via the fixed Ising coupling term, become more challenging, requiring more complex pulse shapes, hence necessitating a larger number of steps  $K$ . It is interesting to note that for this system we had no trouble finding solutions to implement the three-qubit gate with fidelity  $\geq 99.99\%$ . A possible solution is shown in Fig. 3(right). Although the pulse profiles appear more complicated, their magnitudes are actually lower than for some of the two-qubit gates, and although  $K = 50$ , the number of switches per time unit is still only 10. Unlike for the previous model Fig. 4(right) shows that the spectral profile and bandwidth of the solutions are much more desirable.

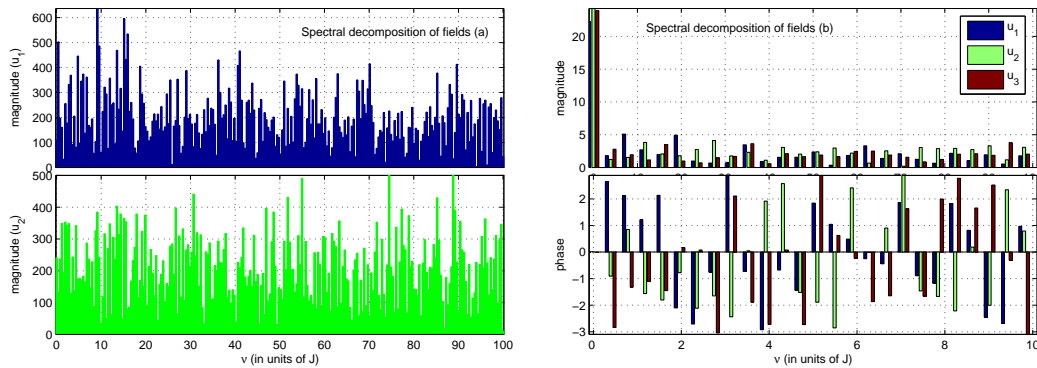


Figure 4. Spectrum of control fields for three-qubit Toffoli-like gate for model system (26) with  $\omega_1 = 10$ ,  $\omega_2 = 12$  and  $\omega_3 = 8$  (left), and model system (28) with  $\Omega = 10$  (right).

## 6. Conclusion

Starting with the most basic control system model commonly used in applications such as (liquid-state) NMR, we have derived more realistic control system models for two types of control of special interest for many applications: (a) control of qubits with fixed inter-qubit coupling using globally applied electromagnetic fields in the regime where off-resonant excitation by the control fields is non-negligible, and (b) control of qubits with fixed coupling using a combination of a fixed globally applied control field and local control electrodes to shift the resonance frequencies of the qubits. Despite the substantially increased complexity of the resulting models, reduced number of independent controls, and non-trivial constraints on the allowed frequency of voltage changes in the latter model, optimal control techniques even in the rather basic form implemented, overall still proved very effective in finding solutions that achieved the target fidelity of 99.99% for almost all cases, although there appears to be scope for further improving the controls with regard to amplitude and bandwidth considerations, and for improving the overall convergence of the algorithm, which even with some of the modifications discussed, appears to be rather slow especially for the three-qubit gates. A somewhat unexpected conclusion of the calculations is that our second model system, which is controlled mainly by local voltage gates that can only alter the detuning of the qubits from the fixed (unmodulated) global field appears to be easier to control, even when constraints on the number of voltage changes are imposed, than the first model system, which is controlled by global fields with arbitrary pulse envelopes.

## 7. Acknowledgements

SGS acknowledges UK research council funding from an EPSRC Advanced Research Fellowship and additional support from the EPSRC QIP IRC and Hitachi. She is currently also a Marie Curie Fellow under the European Union Knowledge Transfer Programme MTDK-CT-2004-509223.

## References

- (1) L. M. K. Vandersypen, I. L. Chuang, *Rev. Mod. Phys.* **76**, 1037 (2004)
- (2) N. Khaneja and S. Glaser, *Chem. Phys.* **267**, 11–23 (2001)
- (3) J. Zhang, J. Vala, S. Sastry, and K. B. Whaley, *Phys. Rev. Lett.* **91** 027903 (2003)
- (4) H. A. Sa Earp and J. K. Pachos, *J. Math. Phys.* **46**, 1 (2005)
- (5) V. Ramakrishna *et al.*, *Phys. Rev. A* **65**(2), 063405 (2002)
- (6) T. Schulte-Herbruggen, A. Sporl, N. Khaneja, S. Glaser, *Phys. Rev. A* **72**(4), 042331 (2005)
- (7) S. G. Schirmer, G. Kandasamy, L. C. L. Hollenberg, *Proceedings of ICCMSE 2007*, AIP Conference Proceedings **963**, Part B, Volume 2 (2007)
- (8) B. E. Kane, *Nature* **393**, 133 (1998)
- (9) D. Loss and D. P. DiVincenzo, *Phys. Rev. A* **57**, 120-126 (1998)
- (10) C. D. Hill *et al.*, *Phys. Rev. B* **72**(4), 045350 (2005)
- (11) G. Kandasamy, C. J. Wellard, L.C.L. Hollenberg, *Nanotechnology* **17**, 4572 (2006)
- (12) L. S. Pontryagin, *The mathematical theory of optimal processes*, (John Wiley & Sons, 1962)
- (13) M. A. Nielsen, I. L. Chuang, *Quantum computing and quantum information* (Cambridge University Press, 2000)
- (14) N. Khaneja, T. Reiss, C. Kehlet, T. S-Herbruggen, S. Glaser, *J. Mag. Res.* **172**, 296-305 (2005)
- (15) S. G. Schirmer, M. D. Girardeau, J. V. Leahy, *Phys. Rev. A* **61**, 012101 (2000)